

<sup>3</sup>Kratsch, K. M., Clayton, F. I., Greene, R. B., Martinez, M., and Wuerer, J. E., "Graphite Ablation in High-Pressure Environments," AIAA Paper 68-1153, Williamsburg, Virginia, Dec., 1968.

<sup>4</sup>Welsh, W. E. and Chung, P. M., "A Modified Theory for the Effect of Surface Temperature on the Combustion Rate of Carbon Surfaces in Air," *Proceedings of the Heat Transfer and Fluid Mechanics Institute*, Stanford University Press, 1963, pp. 146-159.

<sup>5</sup>Segletes, J. A., "Oxidation of POCO AXF-Q1 Graphite in Air," *Journal of Spacecraft and Rockets*, Vol. 10, Dec. 1973, pp. 803-806.

<sup>6</sup>Lincoln, K. A., Howe, J. T. and Liu, T., "Assessment of Chemical Nonequilibrium for Massively Ablating Graphite," *AIAA Journal*, Vol. 11, Aug. 1973, pp. 1198-1200.

<sup>7</sup>Lees, L., "Convective Heat Transfer with Mass Addition and Chemical Reactions," *Third AGARD Colloquium*, March 1958.

<sup>8</sup>Adams, M. C., "Recent Advances in Ablation," *ARS Journal*, Vol. 29, Sept. 1959, pp. 625-632.

<sup>9</sup>JANNAF Thermochemical Tables, 2nd ed., U.S. Department of Commerce, National Bureau of Standards, NSRDS-NBS 37, June 1971.

<sup>10</sup>Lundell, J. H. and Dickey, R. R., "Graphite Ablation at High Temperatures," *AIAA Journal*, Vol. 11, Feb. 1973, pp. 216-222.

## Scheme to Improve Limit Cycle Performance of an Attitude Control System

R. N. Clark\* and P. Dumast†  
University of Washington, Seattle, Wash.

and

D. C. Fosth‡  
Boeing Aerospace Company, Seattle, Wash.

FIGURE 1 is a block diagram of a single axis attitude control system in which an attitude signal,  $\theta^*$ , is derived by integrating the signal from a precision rate gyro. A stabilizing signal  $\epsilon^*$  is also derived in the computer

$$\epsilon^* = K_R \omega^* + K_P \theta^*$$

where

$$\theta^* = \int \omega^* dt$$

$\epsilon^*$  is used to determine the times at which the thruster is fired, the direction of the thrust, and the duration of the thrust pulse. These three items of intelligence are represented as the valve command,  $\tau_c$ , in the diagram. The thruster is characterized by the strength of the thrust,  $A$  (assumed constant during the pulse), a time delay  $\tau_D$  between the instant a turn-on command is received and the instant thrust actually occurs, and a minimum time,  $\tau_o$ , which the pulse width modulator may command as thruster on-time.  $\omega$  is the angular rate of the vehicle about its controlled axis and is related to the thrust  $M$  in the usual way:  $M = J\dot{\omega}$ . The gyro output signal  $m_g$  is dynamically related to the vehicle rate by

$$\ddot{\omega}_g + (2\zeta\omega_n)\dot{\omega}_g + (\omega_n^2)\omega_g = (\omega_n^2)\omega$$

Received October 21, 1974; revision received January 14, 1975.

Index category: Spacecraft Attitude Dynamics and Control.

\*Professor of Electrical Engineering. Also Consultant, Boeing Aerospace Co., Sensors, Guidance, and Control Dept.

†Graduate Student of Electrical Engineering.

‡Engineering Manager, Sensors, Guidance, and Control Dept.

where  $\zeta$  is the damping ratio and  $\omega_n$  the undamped natural frequency of the output axis of the gyro.  $T$  is the cycle time of the computer, and the analog to digital conversion is represented by a zero order hold, the output of which is  $\omega_g^*$ , a piecewise constant representation of  $\omega_g$ .

A conventional method of control for this system is to program the computer to issue a thruster command at each sample instant. The pulse width command at instant  $t_k$  is determined from  $\epsilon^*(t_k)$  according to the curve in Fig. 2. A dead zone of total width  $2W$  is employed to prevent the valve from responding to noise which might exist on the  $\epsilon^*$  signal. The parameters  $W$ ,  $S$ ,  $K_R$ ,  $K_P$ ,  $T$ ,  $\zeta$ , and  $\omega_n$  may then all be adjusted to provide acceptable performance of the system where  $\tau_D$ ,  $\tau_o$ ,  $A$ , and  $J$  are considered fixed.

Insofar as limit cycle performance is concerned these seven parameters are adjusted to minimize control fuel expenditure (total valve on-time) while maintaining acceptable limits on the excursions of  $\omega$  and  $\theta$  during the limit cycle oscillation. The conventional control scheme described above leads to a certain optimum limit cycle performance represented qualitatively by the  $\epsilon^*(t)$  signal in Fig. 3. Here that portion of the limit cycle during which  $\epsilon^*(t)$  reaches its peak is shown. Prior to  $t_o$  the vehicle is drifting at a constant rate.  $t_o$  is the sample instant at which  $\epsilon^*(t)$  first exceeds the dead-zone value  $W$ . A pulse width is calculated from Fig. 2 and a thruster command is issued as soon as this calculation is completed. There is a delay,  $\tau_D$ , between the initiation of the thruster command and the actual occurrence of thrust. Also, the gyro does not

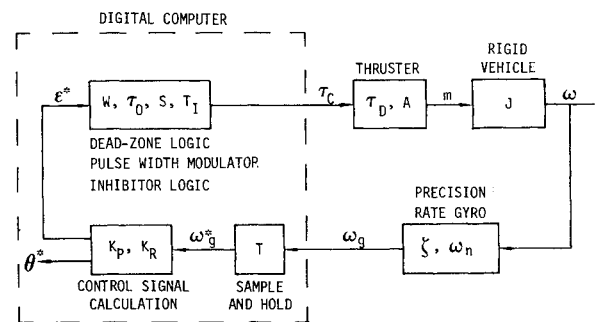


Fig. 1 Single axis attitude control system.

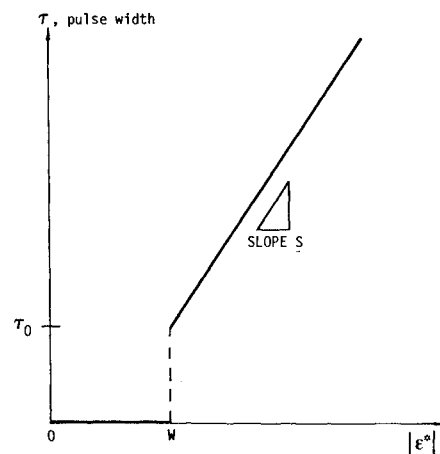
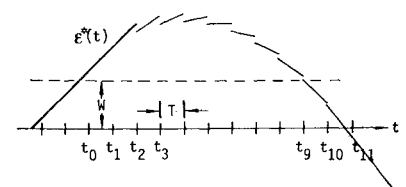


Fig. 2 Pulse-width modulation.

Fig. 3  $\epsilon^*(t)$  vs  $t$  during its reversal.



respond instantly to vehicle motions. Consequently the  $\epsilon^*(t)$  signal continues to increase at a constant rate until  $t_1$ . At instant  $t_1$ , a new pulse width is calculated which will be longer than that calculated at  $t_0$ , and this now becomes the thruster command. Assuming that  $\tau_0$  is longer than  $T$ , this simply means that at  $t_1$  the thruster command is continued. Because of the thruster delay, the gyro dynamics, and the sample and hold operation, the  $\epsilon^*(t)$  signal will remain unaffected by the vehicle acceleration caused by the thruster for some time after  $t_1$ . The thruster will actually come on at time  $t_0 + \tau_D$ , which would be sometime around  $t_1$ , if  $T$  and  $\tau_D$  are approximately the same. Here we show  $\epsilon^*(t)$  increasing at its constant rate until  $t_2$ , the sample instant at which the effect of the thruster is first sensed at the pulse width modulator.  $\epsilon^*(t_2)$  is even larger than  $\epsilon^*(t_1)$ , however, so the pulse width calculated at  $t_2$  will be longer than that at  $t_1$ , and the thrust command will be continued.  $\epsilon^*(t)$  will therefore remain above the dead-zone level for several sample periods. Here it drops below  $W$  for the first time at  $t_{10}$ , so at  $t_{10}$  the thrust command is set to zero. At some later instant, shown at  $t_{11}$  here,  $\epsilon^*(t)$  will be in the dead-zone and decreasing at a constant rate.

The thruster pulse duration during this reversal in  $\epsilon^*(t)$  is much longer than the minimum thruster on time because of the time delays in the control loop. Therefore, the vehicle rate during the limit cycle oscillation is higher than the minimum which is physically possible, so the limit cycle is less efficient than is physically possible.

A new control law, designed to overcome the effects of the time lag and improve the limit cycle performance, has been devised. This scheme utilizes the logical capabilities of the digital computer in addition to its computational abilities, and is called the inhibitor model of control.<sup>1</sup>

The basic inhibitor mode works during the limit cycle in the following way. Referring to Fig. 3, at  $t_0$  the pulse width is calculated and the thruster command issued in the same manner as in the conventional scheme described. In the case shown here, this pulse width will be slightly larger than the minimum  $\tau_0$  because  $\epsilon^*(t_0)$  happens to be slightly greater than  $W$ . At the time the pulse command is issued the computer switches into the "inhibit" mode, which simply means that  $\epsilon^*(t)$  will be ignored (assumed to be zero) for a given period of time—on the order of a few cycle periods. The pulse which is commanded at  $t_0$  will be emitted, the vehicle will decelerate and reverse direction, and the gyro will react and cause  $\epsilon^*(t)$  to reverse direction and even drop below the threshold level  $W$  during the period of inhibition. When the inhibit period is completed, the computer reverts to its alert mode and will command a corrective pulse the next time  $\epsilon^*$  exceeds the threshold level.

To investigate the feasibility of the inhibitor scheme, a simulation of the system shown in Fig. 1 was established. For this simulation, the parameter values shown in Table 1 were used.  $T_I$  is the inhibit period. In each case reported here, a two-pulse limit cycle, symmetrical in  $\omega$ , was established. The results of these tests are summarized in Fig. 4 where the pulse duration which resulted in each case is plotted against the  $K_R$

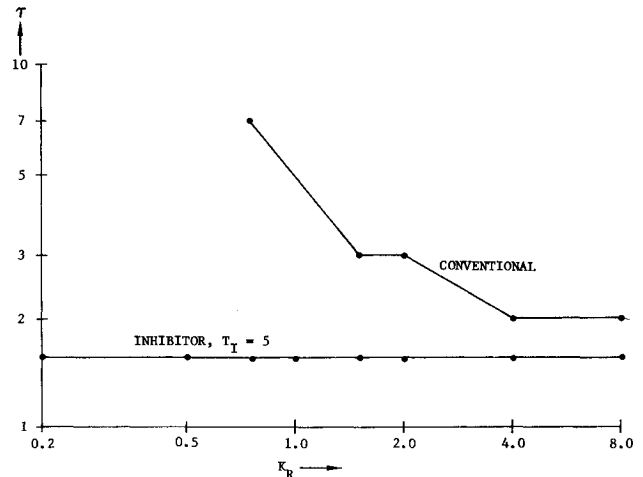


Fig. 4 Pulse-width vs  $K_R$  for  $K_P = 0.2$ .

gain used. In the conventional case the limit cycle was unstable (or did not exist) for  $K_R < 0.5$ .

For a symmetrical limit cycle, the important performance parameters can be established from  $\tau$ . In most attitude control systems the positional accuracy is essentially determined by the dead-zone width  $W$ , so is independent of  $\tau$ . The long-term fuel expenditure is proportional to  $\tau^2$ , so if this is taken as the performance measure, we see that the inhibitor scheme, in the system tested here, gave an improvement in performance over the conventional control law ranging from 20.4 to 1.7, depending on  $K_R$ .

There are many possible variations of the basic inhibitor scheme which is described here. Stability of two pulse limit cycles and the existence of higher order limit cycles are important considerations in any extensions of the inhibitor idea. In the presence of disturbance torques, a situation not investigated here, it would probably be necessary to provide for a variable inhibit period  $T_I$  to prevent excessive excursions of  $\omega$ .

## References

- <sup>1</sup>Dumas, P., "Performance and Stability Analysis of a Digital Pulse Width Modulated Control System," MSEE Thesis, Dept. of Electrical Engineering, Univ. of Washington, Seattle, Wash., 1974.

## Velocity of Bodies Powered by Rapidly Discharged Cold-Gas Thrusters

M. D. Bennett\*

Sandia Laboratories, Albuquerque, N.Mex.

## Nomenclature

$c_i$	= initial sound speed	(m/sec)
$I_s$	= specific impulse	(m/sec)
$k$	= specific-heats parameter, $k = 2/(\gamma - 1)$	
$m_f$	= final vehicle mass	(kg)

Received November 14, 1974; revision received January 20, 1975. This work was supported by the U.S. Energy Research and Development Administration.

Index categories: Missile Systems; Fuels and Propellants, Properties of.

\*Member of Technical Staff, Aerodynamics Projects Department, Associate Fellow AIAA.

Table 1 Parameter values used in simulation

$\tau_D$	= 1
$A$	= 0.02
$J$	= 1
$\omega_n$	= 1.2
$\zeta$	= 0.7
$T$	= 1
$K_P$	= 0.2
$K_R$	= variable, see Fig. 4
$W$	= 1
$\tau_0$	= 1.5
$S$	= 1
$T_I$	= 0 for conventional control law
$T_i$	= 5 for inhibitor mode